RESEARCH ARTICLE

Stimuli-Responsive Properties on a Bisbenzofuropyrazine Core: Mechanochromism and Concentration-Controlled Vapochromism

Shotaro Nakamura,[a] Kohei Okubo,[a] Yuji Nishii,[a] Koji Hirano,*[a, b] Norimitsu Tohnai,*[a] and Masahiro Miura[b]

[a] S. Nakamura, K. Okubo, Dr. Y. Nishii, Prof. Dr. K. Hirano, Prof. Dr. N. Tohnai
Department of Applied Chemistry
Graduate School of Engineering, Osaka University
Suita, Osaka 565-0871 (Japan)
E-mail: k_hirano@chem.eng.osaka-u.ac.jp
tohnai@chem.eng.osaka-u.ac.jp

[b] Prof. Dr. K. Hirano, Prof. Dr. M. Miura
Innovative Catalysis Science Division
Institute for Open and Transdisciplinary Research Initiatives (ICS-OTRI), Osaka University
Suita, Osaka 565-0871 (Japan)

Abstract: Stimulus-responsive organic materials with luminescence switching properties have attracted considerable attention for their practical applications in sensing, security, and display devices. In this paper, bent-type bisbenzofuropyrazine derivatives, **Bent-H** and **Bent-*s*Bu**, with good solubilities were synthesized, and their physical and optical properties were investigated in detail. **Bent-H** gave three crystalline polymorphs, and they showed different luminescence properties depending on their crystal packing structures. In addition, **Bent-H** exhibited mechanochromic luminescence in spite of its rigid skeleton. **Bent-sBu** exhibited unique concentration-dependent vapochromic luminescence. Ground **Bent-*s*Bu** was converted to blue-emissive, green-emissive, and green-emissive high-viscosity solution states at low, moderate, and high concentrations of $CHCl_3$ vapor, respectively. This finding represents a concentration-dependent multi-phase transition with an organic solvent, which is of potent interest for application in sensing systems.

Introduction

Fundamental and applied research has been conducted in sensing and security on external-stimulus-responsive materials with luminescence-switching properties.[1] Materials that exhibit luminescent color changes in response to external stimuli such as light, shear stress, heat, and solvent vapor are known as photochromic, mechanochromic, thermochromic, and vapochromic luminescent materials, respectively.[2] Mechanochromic luminescence refers to a color change of the emission induced by external mechanical stimuli.[2b,d,3] Emissive materials capable of exhibiting mechanochromic luminescence have recently attracted great attention for their application as sensors and memory chips.[4] An increasing number of mechanochromic luminescent materials have been reported to date, and most of them usually rely on flexible structures with rotational parts in their molecular skeletons. Vapochromic luminescent materials are also intriguing as they alter the luminescent color using specific solvent molecules, making them potential candidates for materials applicable to gas sensors and security inks.[5] Many vapochromic active molecules also have been developed.[6] However, almost all undergo just one-color change during the vapochromic process. Consequently, vapochromic materials showing two or more color changes within a single solvent molecule are limited. Recently, Yang and coworkers reported two types of luminescence switching through a two-step phase transition, taking advantage of the difference in the phase transition speed.[7] Yang, Jiang, and coworkers also achieved luminescence switching depending on solvent vapor concentration to induce phase transitions.[8] Despite these certain advancements, luminescence switching by solvent vapor concentration still remains underdeveloped.[9]

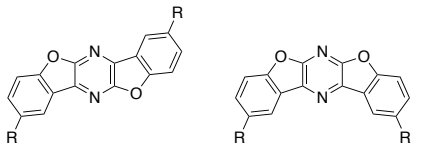

Figure 1. Structures of linear- and bent-type bisbenzofuropyrazines.

Recently, we have synthesized several thermally stable bisbenzofuro[2,3-*b*:2',3'-*e*]pyrazine derivatives by the palladium-catalyzed intramolecular double cyclization (Figure 1, **Linear-R**).[10] In particular, 2,8-di-*tert*-butyl-bisbenzofuro[2,3-*b*:2',3'-*e*]pyrazine formed two different crystal polymorphs and exhibited self-healing mechanochromic properties. Moreover, their bent-type isomers, bis(benzofuro)[2,3-*b*:3',2'-*e*]pyrazines (**Bent-R**), were also synthesized, and parent unsubstituted bis(benzofuro)[2,3-*b*:3',2'-*e*]pyrazine (**Bent-H**) was found to be a good phosphorescent emitter in a dispersed state.[11,12]

In this paper, we report detailed physical and optical properties of **Bent-H** and newly synthesized *sec*-butylated bis(benzofuro)[2,3-*b*:3',2'-*e*]pyrazine (**Bent-*s*Bu**). Compared to the linear-type bis(benzofuro)[2,3-*b*:2',3'-*e*]pyrazines (**Linear-R**), these bent-type isomers are soluble in various solvents, such as chloroform and ethyl acetate, owing to their reduced symmetry. Given the fact that functional materials are widely used in wearable devices and their mass production is thus essential, the high solubility is quite beneficial to allow the low-energy and high-volume production as well as the wet process with reusable solvents for device fabrication by avoiding the expensive and energy-consuming traditional vacuum deposition technique. [13,14,15,16] Furthermore, they exhibited the mechanochromic and vapochromic luminescence. In particular, **Bent-*s*Bu** uniquely showed the concentration-dependent consecutive vapochromic luminescence: the blue and green colors are observed at low and high vapor concentrations, respectively. This is one of rare successful examples of multi-step phase transitions with single organic solvent vapor, which is significant advantage for applications such as chemical sensors.[17] Additionally notable is the mechanochemical property despite their highly rigid and planar structures.

Results and Discussion

Bisphenoxypyrazine derivatives were synthesized by the aromatic nucleophilic substitution reaction of 2,6-dichloropyrazine with two equiv. of ortho-bromophenol derivatives in the presence of K_2CO_3. Subsequently, bisbenzofuropyrazine derivatives **Bent-H** and **Bent-*s*Bu** were obtained by the intramolecular double cyclization using $PdCl_2(PPh_3)_2$ as the catalyst and PivOK as the base, respectively (Scheme 1).

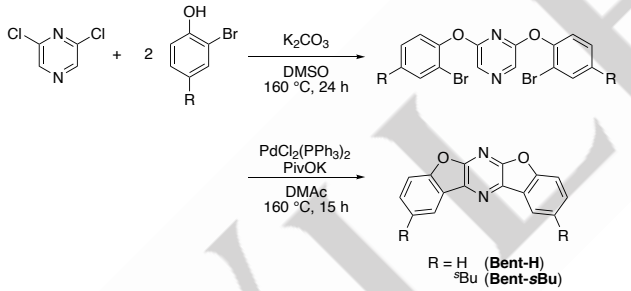

Scheme 1. Synthetic routes to bent-type bisbenzofuropyrazines.

The optical properties of the synthesized compounds were measured in $CHCl_3$ solution (1×10^{-5} M; Figure S1).

Both compounds exhibited absorption spectra with maximum wavelength at 260 and 370 nm and strong emissions with a peak around 400 nm. A slight red shift was observed in both the absorption and emission spectra of **Bent-*s*Bu** compared with those of **Bent-H**. The luminescence quantum yields of **Bent-*s*Bu** and **Bent-H** were moderate values of 0.43 and 0.37, respectively. These results suggest that substitution with alkyl groups had little effect on the photophysical properties in the dispersed state. To investigate the luminescence properties in the aggregation state, each molecule was recrystallized using various methods and conditions. The previously reported linear-type bis(benzofuro)[2,3-*b*:2',3'-*e*]pyrazine without any substituents (R = H in **Linear-R**, Figure 1) was too insoluble to be recrystallized. [10] However, the bent-type **Bent-H** was soluble in various organic solvents even without side chains. Such a high solubility not only enhances their productivity but also allows for wet process applications.[15] **Bent-H** afforded three crystal polymorphs dependent on recrystallization conditions: a colorless block crystal (Form 1 of **Bent-H**), a colorless needle crystal (Form 2 of **Bent-H**), and yellowish-green prism crystal (Form 3 of **Bent-H**) were obtained by slow evaporation from toluene solution, slow evaporation from THF solution, and slow evaporation from CH_2Cl_2 solution, respectively. Variable temperature powder X-ray diffraction (PXRD) showed that Form 2 and Form 3 underwent a phase transition to Form 1 at ca. 130 °C (Figure S2b and c). However, no such phase transition was observed for Form 1 until it reached its melting point (Figure S2a). These results indicate that Form 2 and Form 3 are metastable structures, and Form 1 is a stable structure. DSC measurements of these crystals further confirmed the phase transition before reaching their melting points (Figure S3). On the other hand, **Bent-*s*Bu** gave only a colorless crystal under any conditions as far as we tested.

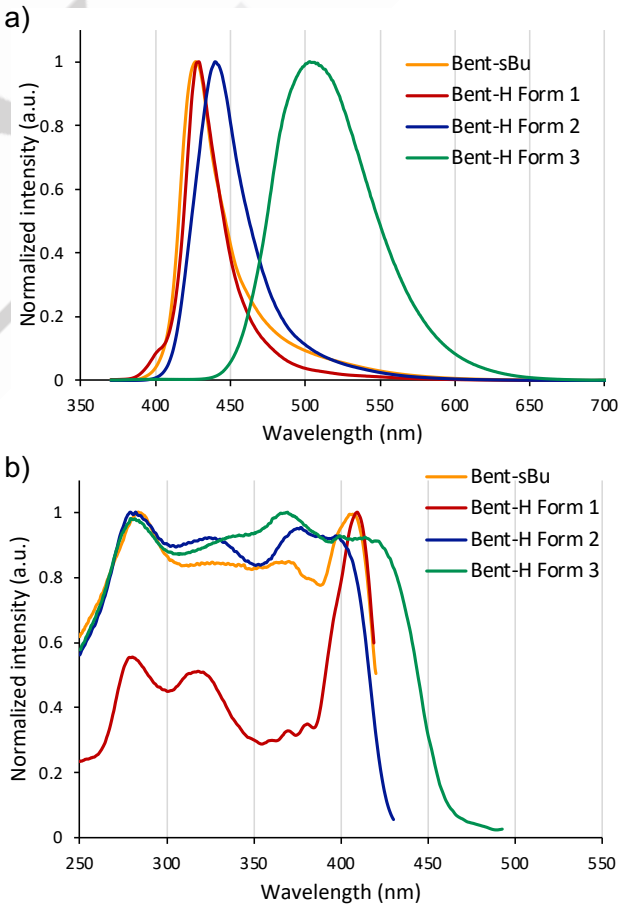

Figure 2. a) Fluorescence spectra of **Bent-*s*Bu**, **Bent-H** Form 1, Form 2 and Form 3. b) Excitation spectra of **Bent-*s*Bu**, **Bent-H** Form 1, Form 2 and Form 3 at each wavelength of maximum emission in the crystalline state.

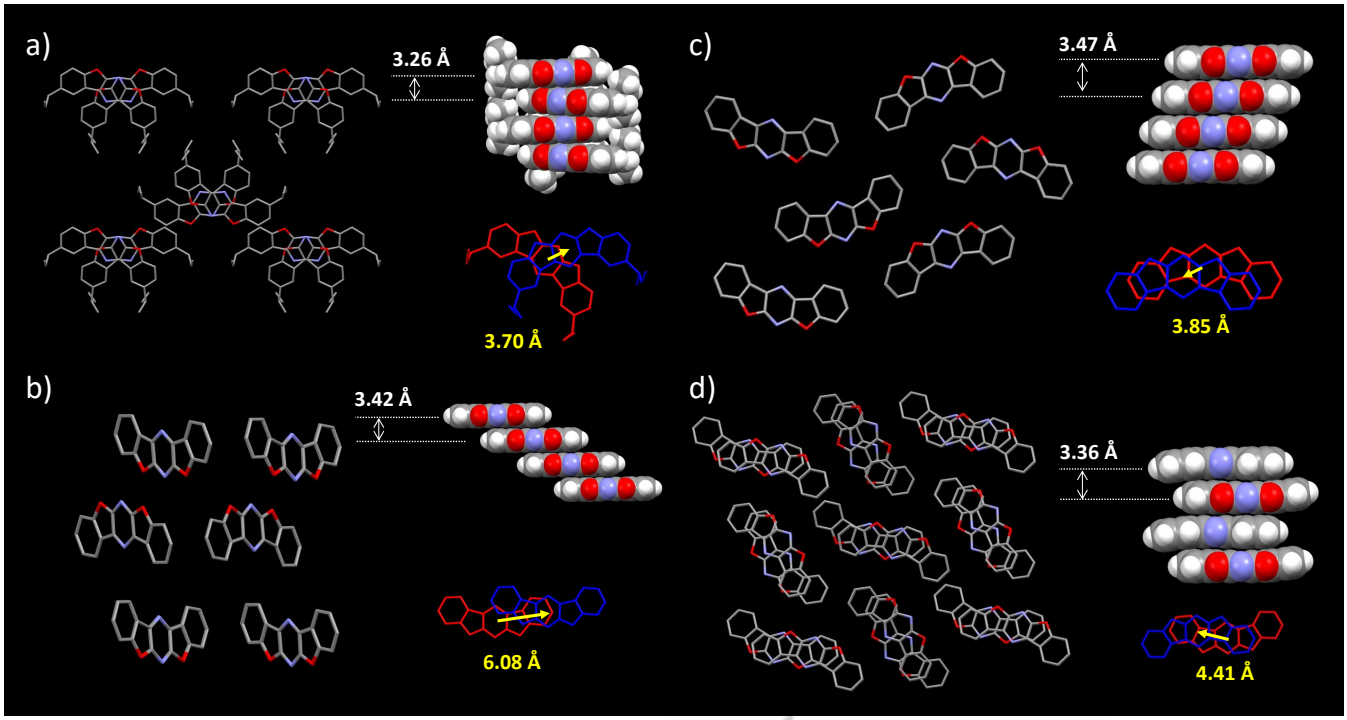

Figure 3. Crystal structures of a) **Bent-sBu**, b) **Bent-H** Form 1, c) **Bent-H** Form 2, and d) **Bent-H** Form 3.

The optical properties of the recrystallized crystals were measured. **Bent-*s*Bu** exhibited monomeric blue emission with a peak at 427 nm (Figure 2a). Similarly, **Bent-H** Form 1 showed strong blue emission with a peak at 429 nm. The fluorescence spectrum of **Bent-H** Form 2 was slightly red-shifted to 440 nm and broadened compared to **Bent-H** Form 1. In sharp contrast, the fluorescence spectrum of **Bent-H** Form 3 was even more red-shifted by 70 nm and broadened, resulting in an emission peak at 503 nm. The similarity in the excitation spectra of Form 1 and Form 2 suggests that they were emitted from the same excited species. The slightly red-shifted and broadened peak observed in Form 2 would arise from its excimer.[18] The emission lifetime of Form 2 (8.02 ns), which is longer than that of Form 1 (1.73 ns), also supports excimer emission, while the colorless crystals of Form 2 indicate no dimeric structure in the ground state. The excitation spectrum of Form 3 was similar to those of Forms 1 and 2 in the region below 410 nm. However, a slightly broadened peak appeared near 425 nm. Thus, Form 3 would exhibit strong intermolecular interactions, leading to dimer formation in the ground state. The ground-state interactions in the Form 3 were also evident from its yellowish-green color of the crystal. The quantum yields of **Bent-*s*Bu**, **Bent-H** Form 1, Form 2, and Form 3 were 0.14, 0.14, 0.45, and 0.41, respectively. The luminescence quantum yields of **Bent-*s*Bu** and **Bent-H** Form 1 were significantly lower than those in solution, whereas **Bent-H** Forms 2 and 3 maintained moderate quantum yields even in the crystalline state.

Single X-ray crystallographic analysis of the obtained crystals was conducted to discuss the luminescence differences dependent on the crystal forms (Figure 3). For **Bent-*s*Bu**, the average distance between the two molecules was 3.26 Å (Figure 3a). The distance between the centers of the pyrazine ring was also relatively short (3.70 Å). Despite its proximity, only monomeric emission was observed from **Bent-*s*Bu**. This is attributed to the stacked arrangement of molecules at an angle, resulting in minimal overlap of the molecular orbitals. Accordingly, the excimer formation is less favored. **Bent-H** Form 1 exhibited a relatively long intermolecular distance of 3.42 Å, with a distance of 6.08 Å between the centers of the pyrazine ring (Figure 3b). The small overlap of the two molecules apparently prevents the excimer formation, resulting in the dominant monomeric luminescence. **Bent-H** Form 2 exhibited a stacked structure, with a large intermolecular distance of 3.47 Å (Figure 3c). However, the distance between the centers of the pyrazine rings was relatively short (3.85 Å), and the degree of overlap was thus relatively large. This structural feature suggests that the two molecules are located at a distance favorable for excimer formation in the excited state while a dimer cannot be formed in the ground state. **Bent-H** Form 3 exhibited an alternating stacking structure of inverted molecules, with a relatively short distance of 3.36 Å between two adjacent molecules and 4.41 Å between their centers of the pyrazine ring (Figure 3d). The close proximity would be responsible for the dimer formation in the ground state, resulting in a red-shifted broad emission.

The obtained crystals showed diverse mechanochromic luminescence properties depending on the substituents. **Bent-*s*Bu** and **Bent-H** Form 1 and Form 2 showed remarkable mechanochromic luminescence properties. **Bent-*s*Bu** exhibited a broad peak at 503 nm upon grinding, and its emission color changed from blue to green (Figure 4a). The original peak at 427 nm almost disappeared. The excitation spectrum of ground **Bent-*s*Bu** at 503 nm was similar to that before grinding at 427 nm, thus indicating that the emission at 503 nm after grinding could originate not from a ground-state dimer but from an excimer. Similar mechanochromic luminescence properties were observed for **Bent-H** Form 1 and Form 2, both of which showed broad

peaks with a maximum at 483 nm (Figures 4b and c). The luminescence lifetimes of **Bent-*s*Bu**, **Bent-H** Form 1, and Form 2 after grinding were 42.95, 45.95, and 47.20 ns, respectively. The considerable increase in the luminescence lifetime suggests the involvement of two molecules in the luminescence after grinding. Such mechanochromic luminescence properties of rigid and unsubstituted condensed aromatic cores deserve significant attention. In contrast, crystals of **Bent-H** Form 3 did not show a luminescence change (Figure 4d). This is probably because of the distinctly strong intermolecular interactions and rigid structure of **Bent-H** Form 3 in the crystalline state, which was also supported by intermolecular potentials in the crystalline state (Figure S4).[19] A slight blue-shift in the excitation spectra was observed for all crystals before and after grinding. PXRD measurements revealed that the crystal structures of these crystals were not retained after grinding (Figure S5).

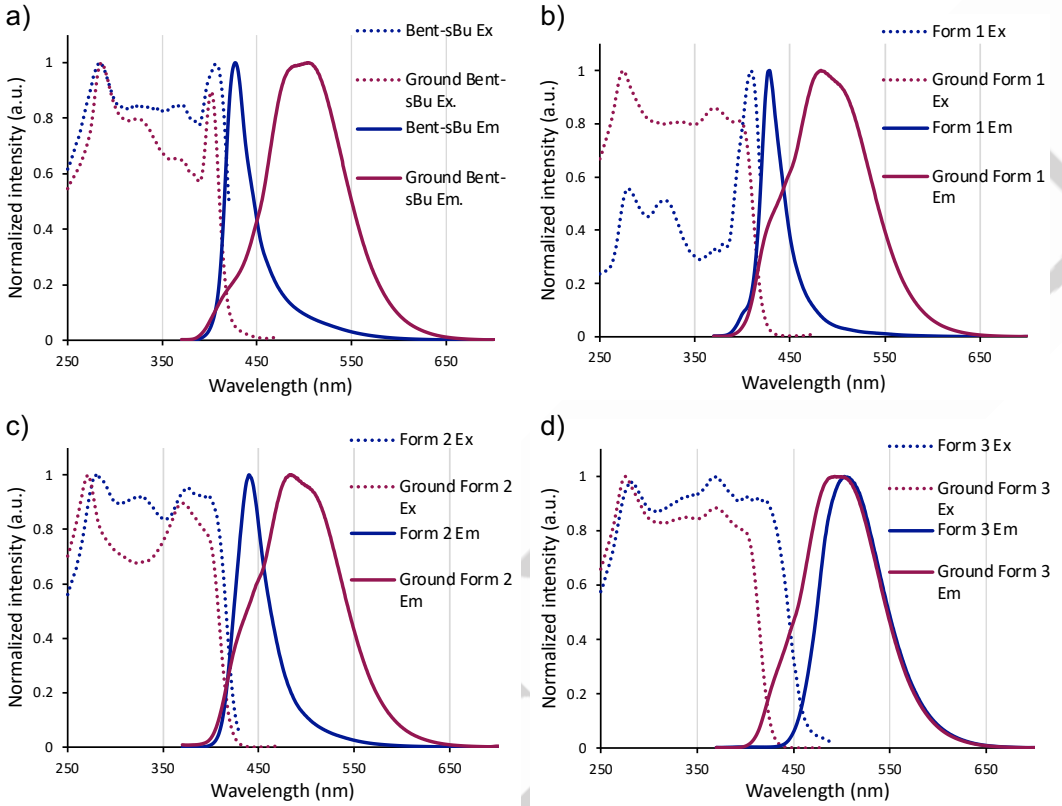

Figure 4. Excitation and emission spectra of as formed crystals and ground crystals of a) **Bent-*s*Bu**, b) **Bent-H** Form 1, c) **Bent-H** Form 2, d) **Bent-H** Form 3.

The behavior of the ground samples was investigated upon exposure to solvent vapors. In particular, **Bent-*s*Bu** exhibited the vapor solvent-dependent unique behavior. When the ground **Bent-*s*Bu** was exposed to ethyl acetate vapor, the emission peak was significantly blue-shifted, and the emission color changed to blue from green (Figure 5a). This phenomenon was reversible, and the original green color was restored by grinding. The reversible process was repeatable at least ten times (Figure S6). On the other hand, exposure to chloroform vapor resulted in an apparent green emission (Figure 5b).

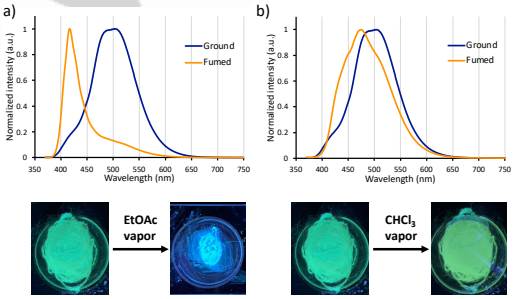

Figure 5. Fluorescence spectra and photographs of ground **Bent-*s*Bu** before and after fuming a) EtOAc, b) $CHCl_3$.

The color change involved three consecutive steps (Scheme 2, and Figure S7). When the ground sample was exposed to chloroform vapor, the emission color first changed to blue (Scheme 2: state Ⅰ′), then to blue-green (Scheme 2: state III), and eventually to clear green (Scheme 2: state IV). State Ⅲ immediately reverted to state Ⅰ′ when exposed to air, whereas state Ⅳ took several hours to revert to state Ⅰ′.

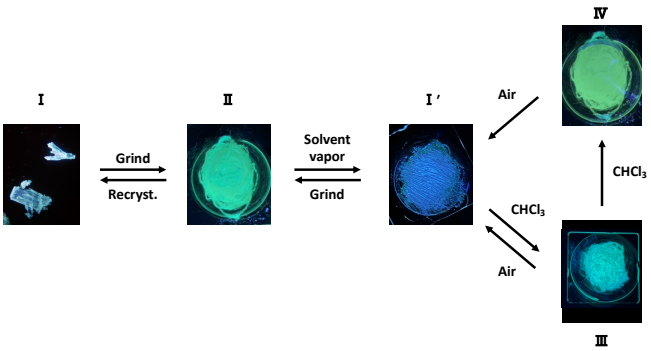

Scheme 2. Overall phase transition process of **Bent-*s*Bu** by various stimuli.

Fluorescence spectroscopy and PXRD measurements were performed to investigate each state (Figure S8). While a slightly

blue-shifted emission peak was obtained for state Ⅰ′ compared with state Ⅰ, the diffraction peak of PXRD was recovered, consistent with the single-crystal peak. State Ⅲ exhibited emission maxima at both 420 and 516 nm, similar to those of state Ⅱ. In state Ⅳ, an only red-shifted, strong peak at 520 nm was obtained and no diffraction peak was observed in the PXRD measurement. The uniform film-like appearance suggests that state Ⅳ is high-viscosity solution state. [20] The emission spectrum of **Bent-*s*Bu** in the solution state was also red-shifted as the concentration increased, which eventually showed the same emission maximum at 520 nm (Figure S9).[21] Therefore, the green emission of state Ⅳ would stem from the high concentration state. Other vapor solvents were also tested. Acetone, hexane, methanol, acetonitrile, and dimethyl sulfoxide showed behaviors similar to ethyl acetate (Figures S10-S14). In contrast, tetrahydrofuran also promoted the consecutive color change identical to that of chloroform (Figure S15). These findings suggest that the first phase transition (Scheme 2: state Ⅱ to state Ⅰ′) is solvent independent while the second phase transition (Scheme 2: state Ⅰ′ to state Ⅲ) is highly solvent-dependent. The solubility of **Bent-*s*Bu** in the solvent is key to controlling the transition. The concentration-dependent clear color change was confirmed by the experiments in Figure 6: As the chloroform vapor concentration (mg/L) increased in a sealed vial, the green luminescence after grinding changed to blue luminescence at low concentration, green luminescence at moderate concentration, and pure green luminescence at high concentration (high-viscosity solution). Moreover, when samples in the green luminescent states (concentration of $CHCl_3$ vapor = 1029–1092 mg/L) were exposed to air, they quickly changed to blue luminescence, same as observed at lower concentrations. Such a rapid color change in responsive to the vapor concentration is highly suggestive of multi-step phase transition, which is not trivial in the literature. [8]

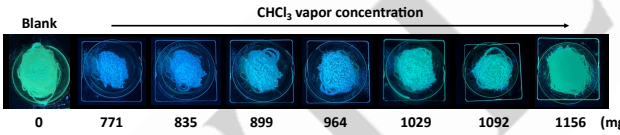

Figure 6. Photographs of ground **Bent-*s*Bu** exposed to $CHCl_3$ vapor at different concentration under UV irradiation at 365 nm. The value below each photo means the concentration of $CHCl_3$ vapor.

The mechanism of aforementioned multi-responsive luminescence is outlined as follows (Scheme 3): Initially, the crystals were crushed by mechanical grinding, resulting in an amorphous state (state Ⅰ to Ⅱ). In subsequent solvent vaporization, the solvent molecules trigger the change of molecular arrangement to recover the packing structure similar to Ⅰ (Ⅱ to Ⅰ′). Relatively poor solvents, including ethyl acetate, acetone, hexane, methanol, acetonitrile, and dimethyl sulfoxide, did not promote any further structural changes. On the other hand, for chloroform and tetrahydrofuran that highly dissolve **Bent-*s*Bu**, solvent molecules are inserted into the molecular packing structure to promote additional phase transition (Ⅰ′ to Ⅲ). Further insertion of solvent molecules eventually causes a loss of regularity, finally leading to a high-viscosity solution state (Ⅲ to Ⅳ). Solvent molecule elimination by exposure to air recovers state Ⅰ′.

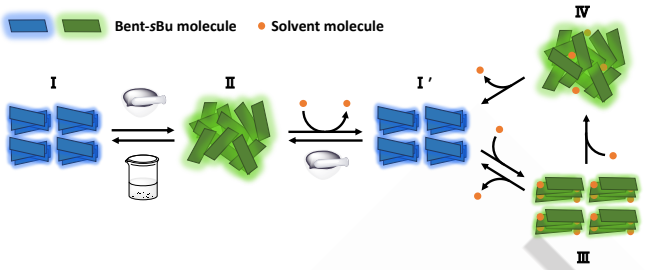

Scheme 3. Illustration of molecular arrangement models using various stimuli.

Forms 1–3 of **Bent-H** were also exposed to chloroform vapor after grinding. All forms exhibited similar blue emission and spectra (Figure S16). This is likely attributed to the loss of crystal structure information during grinding and solvent vapor. The PXRD measurements also suggest that all forms were nearly amorphous after chloroform vaporization (Figure S17). These mechanochromic and vapochromic luminescence were attributed to the central pyrazine ring in **Bent-H** and **Bent-*s*Bu** because the corresponding pyridine analogues, which were previously reported by our group,[22] did not show such properties.[23]

Conclusion

In summary, we report the synthesis of bent-type bis(benzofuro)[2,3-*b*:3',2'-*e*]pyrazines, unsubstituted **Bent-H** and *sec*-Bu-substituted **Bent-*s*Bu**, by a palladium-catalyzed direct arylation reaction. The obtained compounds showed similar luminescence properties in solution, regardless of substituent pattern. However, they exhibited distinct luminescent properties in the crystalline state. **Bent-H** formed three crystalline polymorphs (Forms 1-3) under different recrystallization conditions, while **Bent-*s*Bu** gave a single crystal under any conditions. Form 1, Form 2, and Form 3 of **Bent-H** exhibited monomer luminescence, slightly red-shifted excimer luminescence, and highly red-shifted dimer luminescence, respectively. **Bent-H** also showed mechanochromic luminescence properties, except for Form 3. On the other hand, **Bent-*s*Bu** exhibited unique vapochromic properties, depending on solvents used and their vapor concentration. These results can contribute to further development of mechanochromic and vapochromic luminescence research fields and accelerate the technological advancement of new light-emitting devices.

Experimental Section

Powder diffraction X-ray analysis: Powder X-ray diffraction (PXRD) patterns were measured by Rigaku Ultima IV using graphitemonochromatized CuKα radiation (λ = 1.54178 Å) at room temperature or upon heating.

Differential scanning calorimeter analysis: Differential scanning calorimeter analysis (DSC) analysis was performed in a

Thermo plus DSC8231 (Rigaku) system under an insert flow of nitrogen (100 mL min^{-1}). The samples were heated with a heating rate of 3°C min^{-1}. Alumina was used as the standard sample for the measurement.

Deposition numbers 2282239 (for **Bent-sBu**), 2282245 (for Form 1 of **Bent-H**), 2282246 (for Form 2 of **Bent-H**), 2282244 (for Form 3 of **Bent-H**) contain the supplementary crystallographic data for this paper. These data are provided free of charge by the joint Cambridge Crystallographic Data Centre and Fachinformationszentrum Karlsruhe Access Structures service.

Acknowledgements

This work was supported by JSPS KAKENHI Grant Nos. JP 22H02077 (Grant-in-Aid for Scientific Research (B), to K.H.) and JP 17H06092 (Grant-in-Aid for Specially Promoted Research, to M.M.) and by JST FOREST Program, Grant Number JPMJFR211X to K.H. as well as by JST SPRING, Grant Number JPMJSP2138 to S.N.

Keywords: fluorescence • heterocycles • mechanochromism • polymorphic luminescence • vapochromism

[1] For selected reviews, see: a) Z. Li, Y. Yin, *Adv. Mater.* **2019**, *31*, 1807061; b) D. Sahoo, R. Benny, N. K. KS, S. De, *ChemPlusChem* **2022**, *87*, e202100322; c) W. Wu, K. Chen, T. Wang, N. Wang, X. Huang, L. Zhou, Z. Wang, H. Hao, *J. Mater. Chem. C*, **2023**, *11*, 2026-2052.

[2] For selected reviews, see: a) M. Bagheri, M. Mizaee, S. Hosseini, P. Gholamzadeh, *Dyes and Pigments* **2022**, *203*, 110322; b) S. Ito, *Chem. Lett.* **2021**, *50*, 649-660; c) Q. Shen, L. Wang, X. Ruan, N. Li, W. Wang, W. Wang, J. Shao, X. Dong, *Adv. Funct. Mater.* **2023**, *33*, 2300023. d) Y. Sagara, S. Yamane, M. Mitani, C. Weder, T. Kato, *Adv. Mater.* **2016**, *28*, 1073-1095.

[3] For selected reviews, see: a) Z. Chi, X. Zhang, B. Xu, X. Zhou, C. Ma, Y. Zhang, S. Liu, J. Xu, *Chem. Soc. Rev.* **2012**, *41*, 3878-3896; b) Z. Ma, Z. Wang, M. Teng, Z. Xu, X. Jia. *ChemPhysChem* **2015**, *16*, 1811-1828; c) C. Wang, Z. Li, *Mater. Chem. Front.* **2017**, *1*, 1274-2194.

[4] Selected examples: a) D. Genovese, A. Aliprandi, E. A. Prasetyanto, M. Mauro, M. Hirtz, H. Fuchs, Y. Fujita, H. Uji-I, S. Lebedkin, M. Kappes, L. D. Cola, *Adv. Funct. Mater.* **2016**, *26*, 5271-5278; b) K. Hisano, S. Kimura, K. Ku, T. Shigeyama, N. Akamatsu, A. Shishido, O. Tsutsumi, *Adv. Funct. Mater.* **2021**, *31*, 2104702. c) J. P. Calupitan, A. Brosseau, P. Josse, C. Cabanetos, J. Roncali, R. Métivier, C. Allain, *Adv. Mater. Interfaces* **2022**, *9*, 2102246. d) L. Casimiro, R. Métivier, B. L. Pioufle, S. Bensalem, C. Allain, *Adv. Mater, Interfaces* **2023**, 2300312.

[5] For selected reviews, see: a) X. Zhang, B. Li, Z.-H. Chen, Z.-N. Chen, *J. Mater. Chem.*, **2012**, *22*, 11427-11441; b) B. Jiang, J. Zhang, J. Q. Ma, W. Zheng, L. J. Chen, B. Sun, C. Li, B. W. Hu, H. Tan, X. Li and H. B. Yang, *J. Am. Chem. Soc.* **2016**, *138*, 738–741.c) E. Li, K. Jie, M. Liu, X. Sheng, W. Zhu, F. Huang, *Chem. Soc. Rev.* **2020**, *49*, 1517-1544.

[6] a) S. P. Anthony, S. Varughese and S. M. Draper, *Chem. Commun*., **2009**, 7500-7502; b) S.-J. Yoon, J. W. Chung, J. Gierschner, K. S. Kim, M.-G. Choi, D. Kim and S. Y. Park, *J. Am. Chem. Soc.* **2010**, *132*, 13675-13683; c) E. Takahashi, H. Takaya, T. Naota, *Chem. Eur. J.* **2010**, *16*, 4793-4082; d) X. Zhang, Z. Chi, X. Zhou, S. Liu, Y. Zhang and J. Xu, *J. Phys. Chem. C* **2012**, *116*, 23629-23638; e) K. Wang, S. Huang, Y. Zhang, S. Zhao, H. Zhang, Y. Wang, *Chem. Sci.*, **2013**, *4*, 3288-3293; f) T. Nishiuchi, K. Tanaka, Y. Kuwatani, J. Sung, T. Nishinaga, D. Kim and M. Iyoda, *Chem. Eur. J.* **2013**, *19*, 4110-4116; g) N. Zhao, M. Li, Y. Yan, J. W. Y. Lam, Y. L. Zhang, Y. S. Zhao, K. S. Wong and B. Z. Tang, *J. Mater. Chem. C* **2013**, *1*, 4640-4646; h) C. Li, X. Luo, W. Zhao, C. Li, Z. Liu, Z. Bo, Y. Dong, Y. Q. Dong and B. Z. Tang, *New J. Chem.* **2013**, *37*, 1696-1699; i) Z.-H. Guo, Z.-X. Jin, J.-Y. Wang and J. Pei, *Chem. Commun.* **2014**, *50*, 6088-6090; j) Z. Lin, X. Mei, E. Yang, X. Li, H. Yao, G. Wen, C.-T. Chien, T. J. Chow and Q. Ling, *CrystEngComm*, **2014**, *16*, 11018-11026; k) T. Ono, M. Sugimoto and Y. Hisaeda, *J. Am. Chem. Soc.* **2015**, *137*, 9519-9522; l) H. Naito, Y. Morisaki, Y. Chujo, *Angew. Chem. Int. Ed.* **2015**, *54*, 5084-5087; *Angew. Chem.* **2015**, *127*, 5173-5176; m) P. Rajamalli, P. Gandeepan, M.-J. Huang and C.-H. Cheng, *J. Mater. Chem. C* **2015**, *3*, 3329-3335; n) K. C. Naeem, A. Subhakumari, S. Varughesec and V. C. Nair, *J. Mater. Chem. C,* **2015**, *3*, 10225-10231; o) H. Tian, P. Wang, J. Liu, Y. Duan and Y. Q. Dong, *J. Mater. Chem. C* **2017**, *5*, 12785-12791; p) Q. Li, H. Zhu, F. Huang, *J. Am. Chem. Soc.* **2019**, *141*, 13290-13294.

[7] H. Liu, Y. Shen, Y. Yan, C. Zhou, S. Zhang, B. Li, L. Ye, B. Yang, *Adv. Funct. Mater.* **2019**, *29*, 1901895.

[8] S. Yang, S. Zhou, H. Li, Y. Nie, H. Xu, W. Liu, J. Miao, Y. Li, G. Gao, J. You, X. Jiang, *ACS Appl. Mater. Interfaces* **2022**, *14*, 16611-16620.

[9] a) Y. Li, G. Li, X. Yang, J. Miao, Y. Nie, S. Yang, W. Liu, Y. Cui, G. Sun, *Spectrochimica Acta Part A: Molecular and Biomolecular Spectroscopy* **2023**, *295*, 122622; b) X. Yu, Y. Zhu, X. Ren, Y. Li, L. Shi, W. Zhang, X. Zhu, X.-Q. Hao, M.-P. Song, *Dyes and Pigments* **2023**, *214* , 111195.

[10] S. Nakamura, N. Tohnai, Y. Nishii, T. Hinoue, M. Miura, *ChemPhotoChem* **2019**, *3*, 46-53.

[11] S. Nakamura, M. Tsuboi, T. Taniguchi, Y. Nishii, N. Tohnai, M. Miura, *Chem. Lett.* **2020**, *49*, 921-924.

[12] M. Tsuboi, S. Nakamura, Y. Nishii, N. Tohnai, M. Miura, *Chem. Lett.* **2022**, *51*, 819-822.

[13] For selected reviews, see: a) Z. Ma, S. Li, H. Wang, W. Cheng, Y. Li, L. Pan, Y. Shi, *J. Mater. Chem. B* **2019**, *7*, 173-197; b) C. Wang, K. Xia, H. Wang, X. Liang, Z. Yin, Y. Zhang, *Adv. Mater.* **2019**, *31*, 1801072; c) Y. Hu, T. Niu, Y. Liu, Y. Zhou, Y. Xia, C. Ran, Z. Wu, L. Song, P. Müller-Buschbaum, Y. Chen, W. Huang, *ACS Energy Lett.* **2021**, *6*, 2917-2943; d) Y. Jia, Q. Jiang, H. Sun, P. Liu, D. Hu, Y. Pei, W. Liu, X. Crispin, S. Fabiano, Y. Ma, Y. Cao, *Adv. Mater.* **2021**, *33*, 2102990; e) C. Zhi, S. Shi, Y. Si, B. Fei, H. Huang, J. Hu, *Adv. Mater. Technol.* **2023**, *8*, 2201161;

[14] a) C. P. Yu, S. Kumagai, T. Kushida, M. Mitani, C. Mitsui, H. Ishii, J. Takeya, T. Okamoto, *J. Am. Chem. Soc.* **2022**, *144*, 11159-11167; b) T. Okamoto, C. P. Yu, C. Mitsui, M. Yamagishi, H. Ishii, J. Takeya, *J. Am. Chem. Soc.* **2020**, *142*, 9083-9096;c) C.-A. Hsieh, G.-H. Tan, Y.-T. Chuang, H.-C. Lin, P.-T. Lai, P.-E. Jan, B.-H. Chen, C.-H. Lu, S.-D. Yang, K.-Y. Hsiao, M.-Y. Lu, L.-Y. Chen, H.-W. Lin, *Adv. Sci.* **2023**, *10*, 2206076; d) S. F. Wang, Y. Yuan, Y.-C. Wei, W.-H. Chan, L.-W. Fu, B.-K. Su, I-Y. Chen, K.-J. Chou, P.-T. Chen, H.-F. Hsu, C.-L. Ko, W.-Y. Hung, C.-S. Lee, P.-T. Chou, Y. Chi, *Adv. Funct. Mater.* **2020**, *30*, 2002173.

[15] For selected reviews, see: x) K. S. Yook, J. Y. Lee, *Adv. Mater.* **2014**, *26*, 4218-4233; W. Xu, H. Li, J.-B. Xu, L. Wang, *ACS Appl. Mater. Interfaces* **2018**, *10*, 25878-25901; x) J. W. Parkm B. H. Kang, H. J. Kim, *Adv. Funct. Mater.* **2020**, *30*, 1904632; x) X.-Y. Zeng, Y.-Q. Tang, X.-Y. Cai, J.-X. Tang, Y.-Q. Li, *Mater. Chem. Front.* **2023**, *7*, 1166-1196.

[16] a) T. Someya, T. Sekitani, S. Iba, Y. Kato, H. Kawaguchi, T. Sakurai, *PNAS* **2004**, *101*, 9966; b) X. Yin, J. Yang, H. Wang, *Adv. Funct. Mater.* **2022**, *32*, 2202071.

[17] For selected reviews, see: a) L. E. Kreno, K. Leong, O. K. Farha, M. Allendorf, R. P. V. Duyne, J. T. Hupp, *Chem. Rev.* **2012**, *112*, 1105-1125; b) S. Wenger, *Chem. Rev.* **2013**, *113*, 3686-3733; c) Y. Shen, A. Tissot, C. Serre, *Chem. Sci.* **2022**, *13*, 13978-14007; d) N. Meher, D. Barman, R. Parui, P. K. Lyer, *J. Mater. Chem. C* **2022**, *10*, 10224-10254; e) M. Khatib, H. Haick, *ACS Nano* **2022**, *16*, 7080-7115; f) H. W. Song, W. Choi, T. Jeon, J. H. Oh, *ACS Appl. Electron. Mater.* **2023**, *5*, 77-99.

[18] a) Y. Mizobe, M. Miyata, I. Hisaki, Y. Hasegawa, N. Tohnai, *Org. Lett.* **2006**, *8*, 4295-4298; b) T. Hinoue, Y. Shigenoi, M. Sugino, Y. Mizobe, I. Hisaki, M. Miyata, N. Tohnai, *Chem. Eur. J.* **2012**, *18*, 4634-4643; c) M. Sugino, Y. Araki, K. Hatanaka, I. Hisaki, M. Miyata, N. Tohnai, *Cryst. Growth Des.* **2013**, *13*, 4986-4992; d) N. Tohnai, M. Sugino, Y. Araki, K. Hatanaka, I. Hisaki, M. Miyata, *Dalton Trans.* **2013**, *42*, 15922-15926; e)

M. Sugino, K. Hatanaka, T. Miyano, I. Hisaki, M. Miyata, A. Sakon, H. Uekusa, N. Tohnai, *Tetrahedron Lett.* **2014**, *55*, 732-736.

[19] a) A. Gavezzotti, *Acc. Chem. Res.* **1994**, *27*, 309; b) A. Gavezzotti, G. Filippini, *J. Phys. Chem.,* **1994**, *98*, 4831-4837.

[20] K. Ishii, K. Yokomori, K. Murata, S. Nakamura, K. Enomoto, *RSC Adv.* **2022**, *12*, 18307-18310.

[21] T. Förster, *Angew. Chem. Int. Ed. Engl.* **1969**, *8*, 333; b] B. J. Birks, *Rep. Prog. Phys.* **1975**, *38*, 903.[22] H. Kaida, T. Goya, Y. Nishii, K. Hirano, T. Satoh, M. Miura, *Chem. Lett.* **2017**, *19*, 1236-1239.

[23] We also investigated temperature-dependent fluorescence spectra of **Bent-H** (Form 1, 2, and 3) and **Bent-*s*Bu** crystals. However, thermochromic luminescence was not observed: the luminescence intensity just decreased for all crystals. Additionally, we conducted powder X-ray diffraction measurement of ground powders of all materials after heating at 100 °C for 10 min. Forms 1–3 of **Bent-H** kept amorphous form even after heating. On the other hand, some original peaks of **Bent-*s*Bu** were recovered after heating. See the Supporting Information for more details.

Entry for the Table of Contents

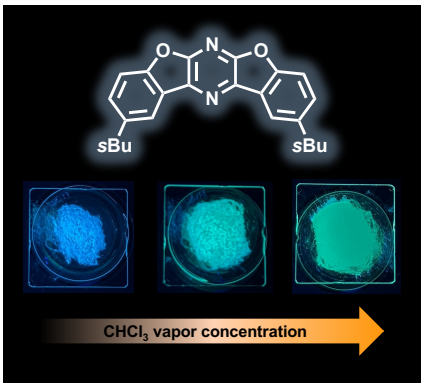

A novel π-core system: bent-shaped bisbenzofuropyrazines were easily synthesized by the palladium-catalyzed intramolecular double cyclization reaction. The unsubstituted derivative shows good solubility in spite of its rigid planar structure and provides three polymorphs with different mechanochromic luminescent properties. A ground sample of the *sec*-butylated derivative exhibits concentration-dependent unique vapochromic luminescent behavior.